

Disclaimer

This document was prepared as an account of work sponsored by the United States Government. Neither the United States Government nor any agency thereof, nor The Regents of the University of California, nor any of their employees, makes any warranty, express or implied, or assumes any legal liability or responsibility for the accuracy, completeness, or usefulness of any information, apparatus, product, or process disclosed, or represents that its use would not infringe privately owned rights. Reference herein to any specific commercial products process, or service by its trade name, trademark, manufacturer, or otherwise, does not necessarily constitute or imply its endorsement, recommendation, or favoring by the United States Government or any agency thereof, or The Regents of the University of California. The views and opinions of authors expressed herein do not necessarily state or reflect those of the United States Government or any agency thereof of The Regents of the University of California and shall not be used for advertising or product endorsement purposes.

Lawrence Berkeley Laboratory is an equal opportunity employer.

1. Introduction

High energy physics today is in an extraordinarily fortunate position. The standard model is reliable but incomplete: it predicts a fifth force for its completion, with new quanta that are no heavier than a few TeV. If that prediction were to fail we would make an equally important discovery: a deeper theory that has successfully hidden behind the standard model until now. This is truly a no-lose situation, *if* we can construct the necessary experimental facilities. While the focus of this talk is on TeV e^+e^- linear colliders, I will also briefly discuss the complementary role of multi-TeV proton-proton colliders. Both e^+e^- and pp colliders are needed for efficient exploration of the new physics in the TeV domain.

This talk is organized in two principal sections. The first is a brief summary of new physics we *might* find at TeV e^+e^- colliders, including the exciting prospect¹ of TeV photon-photon collisions using the back-scattered laser technique first applied in a photoproduction experiment at SLAC.² If it proves practicable, photon-photon scattering could rival e^+e^- annihilation in importance. In addition to standard processes, I will discuss high energy $\gamma\gamma \rightarrow ZZ$ scattering as a probe of ultraheavy quanta too heavy to produce directly.³

The second section of the talk concerns what we *must* find, the physics of electroweak symmetry breaking, in the form of Higgs bosons below 1 TeV or strong WW scattering above 1 TeV. In particular, I will present a rough estimate of the strong WW scattering signal as a function of collider energy.

This introduction will conclude with brief discussions of three topics:

- a general framework for the fifth force,
- energy and luminosity requirements for TeV e^+e^- colliders,
- the physics environment at TeV e^+e^- colliders.

1.1 THE FIFTH FORCE: A GENERAL FRAMEWORK

The symmetry breaking sector for the $SU(2)_L \times U(1)_Y$ gauge interactions is specified by a lagrangian \mathcal{L}_{SB} describing the new force and the associated new quanta. Though we do not know the details of the new force or quanta, we

do know they must have certain general properties in order to accomplish their symmetry breaking mission:⁴⁾

- \mathcal{L}_{SB} must possess a global symmetry G that breaks spontaneously to a subgroup H , giving rise to at least three Goldstone bosons denoted w^+, w^-, z .
- The Goldstone bosons w^\pm, z couple to the $SU(2)_L \times U(1)_Y$ gauge currents, with a dimensionful coupling strength

$$v = (\sqrt{2}G_F)^{-1/2} \cong \frac{1}{4} \text{ TeV} \quad (1.1)$$

analogous to the coupling of the pion to the hadronic axial current with strength $F_\pi = 92 \text{ MeV}$. By means of the Higgs mechanism the $SU(2)_L \times U(1)_Y$ gauge interactions transmuted w^\pm, z into the longitudinal gauge boson polarization modes W_L^\pm, Z_L .

- The equivalence theorem, proved initially in tree approximation⁵ and then to all orders^{6,7} (proof to all orders is essential if the fifth force is strong), asserts the equality of high energy W_L scattering to the (unphysical but calculable) scattering of the related Goldstone bosons in an R_ξ gauge,

$$\begin{aligned} \mathcal{M}(W_L(p_1), W_L(p_2) \dots) &= \mathcal{M}(w(p_1), w(p_2) \dots) \\ &+ O(M_W/E_i). \end{aligned} \quad (1.2)$$

Therefore by observing the interactions of the longitudinal gauge boson modes at high energy we are actually studying the physics of \mathcal{L}_{SB} . We are using the fact that W_L^\pm, Z_L are not quanta of the gauge sector but are in effect citizens of \mathcal{L}_{SB} .

- Gauge invariance requires the global symmetries of \mathcal{L}_{SB} to be at least as big as the gauge groups, $G \supset SU(2)_L \times U(1)_Y$ and $H \supset U(1)_{EM}$. In the absence of other light quanta than W_L, Z_L , this property implies low energy theorems⁸ (first proved under more restrictive conditions⁶), e.g., for $W_L^+ W_L^- \rightarrow Z_L Z_L$ in the $J = 0$ partial wave

$$a_0(W_L^+ W_L^- \rightarrow Z_L Z_L) = \frac{1}{\rho} \frac{s}{16\pi v^2} \cong \frac{s}{(1.8 \text{ TeV})^2} \quad (1.3)$$

where $\rho = (M_W/M_Z \cos \theta_W)^2$ and equation (1.3) is valid in the energy domain $M_W^2 \ll s \ll \min\{M_{SB}^2, (4\pi v)^2\}$ where M_{SB} is the typical mass scale of the quanta of \mathcal{L}_{SB} . The analogous low energy theorem for pion scattering is⁹

$$a_0(\pi^+\pi^- \rightarrow \pi^0\pi^0) = \frac{s}{16\pi F_\pi^2} \cong \frac{s}{(700 \text{ MeV})^2} \quad (1.4)$$

- Unitarity requires the linear growth in s to be cut off eventually. The location of the cutoff determines whether \mathcal{L}_{SB} is weak or strong and whether it is a Higgs boson theory or a theory of a more complicated, strongly interacting set of particles.

In particular the cutoff typically occurs at a scale of order M_{SB} , so that at and above the cutoff (until significant inelasticity sets in) we have

$$|a_0(W_L^+W_L^- + Z_L Z_L)| \cong \frac{O(M_{SB}^2)}{16\pi v^2} \cong O\left(\frac{M_{SB}}{1.8 \text{ TeV}}\right)^2 \quad (1.5)$$

There are then two possibilities:

- $M_{SB} \ll 1.8 \text{ TeV}$. \mathcal{L}_{SB} is weak and there are narrow Higgs bosons. Then $M_{SB} = m_H$ if there is just one Higgs boson or $M_{SB} = \sqrt{\langle m_H^2 \rangle}$ is an appropriately weighted average if there is more than one Higgs boson.
- $M_{SB} \cong O(1.8 \text{ TeV})$. \mathcal{L}_{SB} is strong and there is strong WW scattering above 1 TeV. New particles including WW resonances are likely between about 1 and 3 TeV.

Yukawa would have enjoyed case ii), since he hypothesized that the pion was the exchange quantum of both weak and strong interactions. In case ii) W is the quantum of weak ($SU(2)_L \times U(1)_Y$) and strong (\mathcal{L}_{SB}) interactions.

A no-lose collider is one at which strong WW scattering can be observed, since we can then learn from the presence or absence of the strong WW scattering signal about the strength of the fifth force and the mass domain of the new quanta. The parameters of a no-lose e^+e^- collider are estimated in section 3.

1.2 COLLIDER REQUIREMENTS: LUMINOSITY AND ENERGY

Since the relatively clean environment of e^+e^- collisions make detailed studies feasible, one requirement is luminosity sufficient to provide data samples large enough for precision studies. This is no easy task, since the annihilation cross section is very small,

$$\sigma|_{R=1} = \frac{4\pi\alpha^2}{3s} = \frac{100 \text{ fb}}{s(\text{TeV}^2)} \quad (1.6)$$

where I use the high energy value $\alpha = 1/128$. If we want $N \geq 5000$ events per unit R we need integrated luminosity $\geq 50 \text{ fb}^{-1} \cdot s(\text{TeV}^2)$ or instantaneous luminosity $\geq 5 \cdot 10^{33} \text{ cm}^{-2} \text{ sec}^{-1} \cdot s(\text{TeV}^2)$ assuming a year of data collection.

Heavy Higgs boson production and strong WW scattering occur by WW fusion (figure 1.1), and are extremely sensitive to the collider energy. The effective W approximation for $W_L W_L$ scattering, analogous to the familiar effective photon approximation of Weiszacker and Williams, implies an effective $W_L W_L$ luminosity¹⁰⁾

$$\frac{\partial \mathcal{L}}{\partial \tau} = \frac{\alpha_W^2}{16\pi} \left[\left(\frac{1}{\tau} + 1 \right) \ln \frac{1}{\tau} + 2 - \frac{2}{\tau} \right] \quad (1.7)$$

where $\tau = s_{WW}/s_{e^+e^-}$. The quantity in square brackets is shown in table 1.1, as a function of $\tau^{-1/2} = \sqrt{s_{e^+e^-}/s_{WW}}$, from threshold at $\tau^{-1/2} = 1$ to $\tau^{-1/2} = 10$.

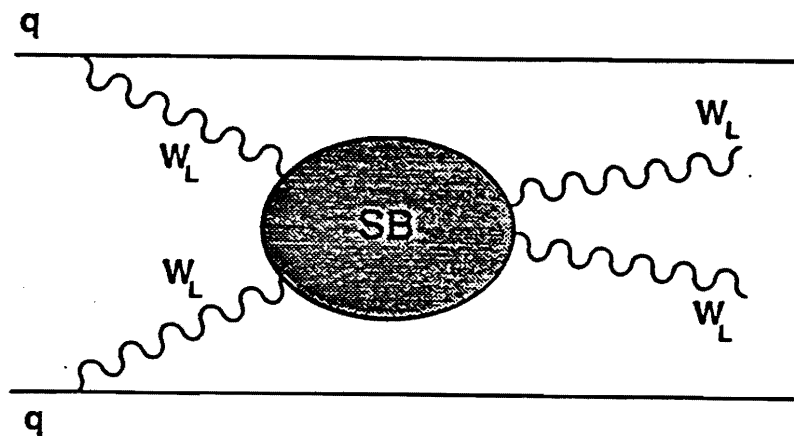


Figure 1.1 WW fusion of longitudinal W bosons via the symmetry breaking interactions \mathcal{L}_{SB} .

$\tau^{-1/2}$	1	1.25	1.5	2	3	4	5	7.5	10
I	0	0.02	0.14	0.9	6.0	17	36	120	270

Table 1.1 The effective luminosity of longitudinal W boson pairs as a function of $\tau^{-1/2} = \sqrt{s_{e^+e^-}/s_{w^+w^-}}$. The quantity I is the luminosity without the prefactor $\alpha_W^2/16\pi$.

The luminosity grows very rapidly in the threshold region. For instance, if we wish to study the WW system at $\sqrt{s_{WW}} = 1$ TeV, a $\sqrt{s_{e^+e^-}} = 3$ TeV collider has $6.0/0.14 = 43$ times greater $W_L W_L$ luminosity than a 1.5 TeV collider! For this particular physics it is very difficult to try to use enhanced luminosity to compensate for low energy, a point that is reinforced by the fact that not only the signal but also the signal:background ratio is more favorable at higher energy. In the study of strong WW scattering with $\sqrt{s_{WW}} > 1$ TeV at the SSC, there are important contributions for $\tau^{-1/2} = \sqrt{s_{qq}/s_{WW}}$ from roughly $\tau^{-1/2} = 3$ to ~ 10 .

1.3 PHYSICS ENVIRONMENT

In some respects the environment at TeV linear e^+e^- colliders begins to resemble pp colliders more than the old familiar e^+e^- storage rings. This is due principally to the beamstrahlung phenomenon¹¹ and to synchrotron radiation created at the final focus.¹² Some important consequences are

- total energy and longitudinal momentum constraints are lost,
- even with the most benign designs, beamstrahlung and initial state radiation induce substantial luminosity loss at the maximum e^+e^- collision energy,
- “auto-scanning”, i.e., all energies below E_{max} can be observed while running at E_{max} , so that for instance a Z' resonance at $M_{Z'} < E_{MAX}$ will be immediately visible without scanning,
- beamstrahlung and synchrotron radiation create a hostile environment along the beam direction, making detection at small angles impossible (say below $5 - 10^\circ$), a more severe constraint than in pp colliders.

Two recent papers have pointed to dangerous minijet¹³ and heavy¹⁴ quark backgrounds that arise from the extreme beamstrahlung $\gamma\gamma$ spectrum that would occur with round beams, as in the curve with unit aspect ratio, $G = 1$, shown in figure 1.2 taken from Blankenbecler and Drell.¹⁵ However Figure 1.2 also shows that with a flat beam, aspect ratio $G = 5$, the beamstrahlung spectrum is very similar to the bremsstrahlung spectrum, and the dangerous backgrounds are mitigated. In particular, Fujii will discuss the minijet background with flat beams in the following talk.¹⁶ These results confirm the wisdom of current design with flat beams. For instance a 1 TeV JLC design¹⁷ calls for beam dimensions of $2.3 (!) \times 370$ nm or $G = (r_x + r_y)/2\sqrt{r_x r_y} = 6.4$.

Despite the phenomena described above, TeV e^+e^- colliders will in substantial measure retain the traditional virtues of e^+e^- physics. These are especially

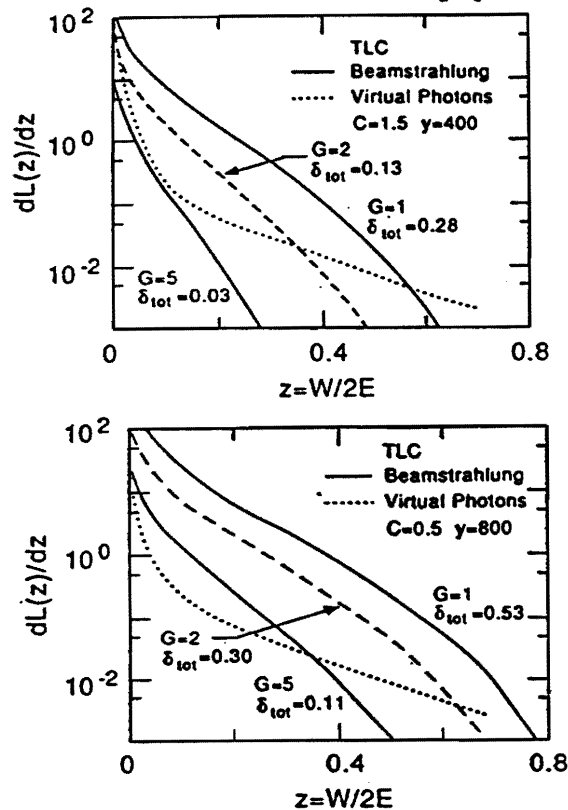


Figure 1.2 Photon-photon luminosity distributions from beamstrahlung for various collider design choices, compared with the photon-photon luminosity from bremsstrahlung (taken from reference 15).

- favorable signal:background ratios, e.g., in annihilation where both new and old physics comes roughly in units of R (ranging from tenths to tens of R units); as a result WW and ZZ pairs are detectable in the four jet final state, inconceivable at pp colliders where both or perhaps only one boson (in “tagged” events¹⁸) must decay leptonically for the pair to be observable,
- backgrounds are precisely calculable since the production mechanisms are electroweak, though with familiar uncertainties when details of hadronization are relevant.

In addition linear colliders should have an important new virtue: the possibility of large longitudinal polarization, that will be a useful analytical tool for a variety of detailed studies.

2. Might find?

In this section I will discuss, very briefly, some of the physics we might find in TeV e^+e^- and $\gamma\gamma$ collisions .

2.1 e^+e^- ANNIHILATION

1) Heavy quarks, leptons, neutrinos

A fourth generation of quarks and leptons is possible, provided the $SU(2)_L$ doublets are sufficiently degenerate to satisfy the rho parameter constraint.¹⁹ Given our ignorance of the origin of quark and lepton masses, we cannot judge whether or not this is a likely possibility. As shown by the SLAC study group,²⁰ there are good signals for quarks and charged leptons over most of the kinematically accessible range.

Buchmüller and Greub²¹ have considered the possibility of observing a heavy Majorana neutrino by

$$e^+e^- \rightarrow \nu N, N \rightarrow \ell W, W \rightarrow \ell \nu. \quad (2.1)$$

Simulation studies would be useful to establish the viability and level of the observable signal.

At the SSC heavy quarks are readily detectable at least to $m_Q = 1 \text{ TeV}$ ²²⁾ but detection of heavy charged leptons²³⁾ is very difficult, perhaps impossible. I am not aware of studies of heavy neutrino detection at pp colliders.

2) Supersymmetry

In e^+e^- annihilation the asymptotic cross sections for squarks and sleptons are half the corresponding quark and lepton cross sections,

$$R(\tilde{f}\tilde{f}) = \frac{1}{2}R(f\bar{f}), \quad (2.2)$$

and they are probably observable at energies sufficiently above threshold to overcome the slow β^3 growth of p -wave phase space. I am not aware of detailed simulations of the signals and backgrounds. At the SSC, gluinos are detectable to $\sim 2 \text{ TeV}$ and squarks to at least $\sim 1 \text{ TeV}$, but sleptons might be unobservable.

If supersymmetric particles such as gluinos or squarks are discovered, we will want to find and study the accompanying Higgs sector. In the minimal model it consists of light and heavy neutral scalars, h and H , a charged scalar H^\pm , and a neutral pseudoscalar A . All could be observed in principle at an e^+e^- collider. The light scalar h resembles the standard model Higgs boson in its production modes and is produced in $e^+e^- \rightarrow Zh$ or Z^*h and in WW fusion, $e^+e^- \rightarrow \bar{\nu}\nu h$. The charged scalar is produced with the usual $\frac{1}{4}\beta^3$ value of R , while the heavy scalar and pseudoscalar are pair produced in $e^+e^- \rightarrow HA$ with²⁴⁾ $R \cong 0.1$ far above threshold. At the LHC or SSC h might be observed in $h \rightarrow \gamma\gamma$ in association with a $\bar{t}t$ pair (like the standard intermediate mass Higgs boson) and H^+ will be observable if $t \rightarrow H^+b$ is kinematically allowed, but I am not aware of any prospects to find H and A .

3) Anomalous interactions

TeV e^+e^- colliders have great sensitivity to anomalous four-fermion interactions involving electrons, as would for instance occur if leptons and quarks are composite. Using a standard convention²⁵⁾ a 1 TeV e^+e^- collider is sensitive to anomalous Bhabha and $e^+e^- \rightarrow \mu^+\mu^-$ scattering to scales of order ten's of TeV.²⁶⁾ In comparison, the SSC can probe anomalous four quark interactions to about $\Lambda = 25 \text{ TeV}$.²⁷⁾

Gauge interaction anomalies can also be sensitively probed in $e^+e^- \rightarrow W^+W^-$. Parity and charge-conjugation invariance fix the form of the lowest

dimension anomalous interactions,²⁸⁾

$$\delta\mathcal{L}_i = (\kappa_i - 1)W_\mu^+W_\nu^-F_i^{\mu\nu} + \frac{\lambda_i}{M_W^2}W_{\mu\sigma}^+W_\nu^-F_i^{\mu\nu} \quad (2.3)$$

for $i = \gamma$ or Z . A simulation assuming 30 fb^{-1} at an 0.5 TeV collider without polarization obtains 90% confidence level constraints of roughly²⁹⁾ $|\kappa_\gamma - 1| < 0.14$ and $|\lambda_\gamma| < 0.4$ (for the precise constraints see the figures of reference 29) assuming $\kappa_Z - 1 = \lambda_Z = 0$. A more recent study assuming polarization, described in Fujii's talk,¹⁶⁾ gives stronger limits. At the SSC with 10 fb^{-1} the 1σ limits would be³⁰⁾ $|\kappa_\gamma - 1| < 0.1$ and $|\lambda_\gamma| < 0.01$, regardless of the values of κ_Z and λ_Z . Since $e^+e^- \rightarrow W^+W^-$ proceeds by both γ and Z exchange the constraints on γ and Z are coupled, but they are independent at pp colliders where the relevant processes $W^* \rightarrow W\gamma$ and $W^* \rightarrow WZ$ probe the γ and Z couplings separately. With e^+e^- colliders independent constraints can be achieved by including $e^+e^- \rightarrow e\nu W$ ³¹⁾ and $\gamma\gamma \rightarrow WW$, the latter discussed below. Fujii will discuss $e^+e^- \rightarrow WW$ in more detail.¹⁶⁾

4) Top quark physics

Unless the top quark surprises us considerably³²⁾ it can be studied at a 1/2 TeV collider. Toponium dynamics will be complex and interesting in the domain where the top quark lifetime is less than or of the order of the bound-state formation time set by QCD. Furthermore, the toponium potential will be sensitive to Higgs boson exchange. A thorough simulation was previously described by Fujii,³³⁾ who will also discuss top quark physics at this meeting.¹⁶⁾

5) Z'

A Z' boson could be our best and perhaps only window to the GUT scale. Finding a Z' with properties predicted by one of the GUT theories would be a spectacular achievement. It would be equally spectacular to find a Z' that does not fit into any known GUT! The cross section would be enormous,

$$\sigma = 1.5 \cdot 10^5 \text{ fb} \cdot \frac{B(Z' \rightarrow ee)}{0.01} \cdot \frac{1}{M_{Z'}^2(\text{TeV})} \quad (2.4)$$

so that detailed studies would be possible with lower luminosity than $10^{33} \text{ cm}^{-2} \text{ sec}^{-1}$. At the SSC the reach for Z' bosons is from 4 to 8 TeV for various possible

models. Discovery of a Z' at the LHC or SSC would be irresistible motivation to build a matched e^+e^- collider.

⋮
⋮

27) *Something no one has imagined*

Skipping the intervening 21 items for lack of time we come to one of the best reasons for building any accelerator. Unfortunately in the TeV era the economics of accelerator construction make it a less sufficient justification than it once was.

2.2 $\gamma\gamma$ Scattering

In backward scattering of a low energy photon from a high energy electron, essentially all of the electron's energy and momentum is transferred to the back-scattered photon. Using laser sources at a linear e^+e^- collider it may be possible to produce high luminosity $e\gamma$ and $\gamma\gamma$ collisions at a large fraction of the initial e^+e^- energy.¹⁾ Here I will discuss $\gamma\gamma$ collisions, that are possible with luminosity equal to or slightly greater than the e^+e^- luminosity of the parent e^+e^- collider. If practicable this technique would enable a rich experimental program that could rival e^+e^- scattering in importance.

The dominant process is $\gamma\gamma \rightarrow WW$ that occurs with a large, asymptotically constant cross section,

$$\sigma = \frac{8\pi\alpha^2}{M_W^2} = 93 \text{ pb} + O\left(\frac{M_W^2}{s}\right) \quad (2.5)$$

or in units of R as defined in equation (1.1)

$$R = \frac{6s}{M_W^2} = 940 \cdot s(\text{TeV}^2). \quad (2.6)$$

The constant cross section results from mass singularities in the forward and backward directions that are regulated by the W mass. Since the forward and backward regions are unobservable, equations (2.5) and (2.6) are somewhat misleading. The cross section for scattering away from the beam direction decreases with energy but is still extremely large in realistic cases of interest. For instance, I find that $4 \cdot 10^5$ WW pairs would be produced with $|\cos\theta_W| < 0.9$ assuming

3 eV lasers scattering from the e^\pm beams of a $\sqrt{s} = 1$ TeV collider with an integrated luminosity corresponding to 50 pb^{-1} of e^+e^- collisions.

Such large numbers suggest the possibility of a “ W factory” in which we could begin to make precision measurements and search for rare decays, like the presently ongoing studies of the Z boson. Thought should be given to the physics motivation for such a program. To encourage such efforts I am announcing the second Chanowitz Prize³⁵⁾: free lunch with Michael Peskin to anyone who either proposes a very interesting measurement for a W factory or argues persuasively that there are no interesting measurements to be made. In the latter case but not in the former the lunch must be in the SLAC cafeteria. A maximum of three prizes will be awarded.

$\gamma\gamma \rightarrow WW$ will of course provide fundamental tests of the electroweak gauge theory, including direct access to the characteristic four-point contact interaction. (The cancellation between the contact interaction and the W exchange graphs gives rise to the peculiar mass singularities that engender the asymptotically constant total cross section.) It is also an excellent process in which to study the anomalous interactions defined in equation (2.3).³⁵⁾ As shown in figure 2.1 taken from Choi and Schrempp,³⁵⁾ $\gamma\gamma \rightarrow WW$ and $e^+e^- \rightarrow WW$

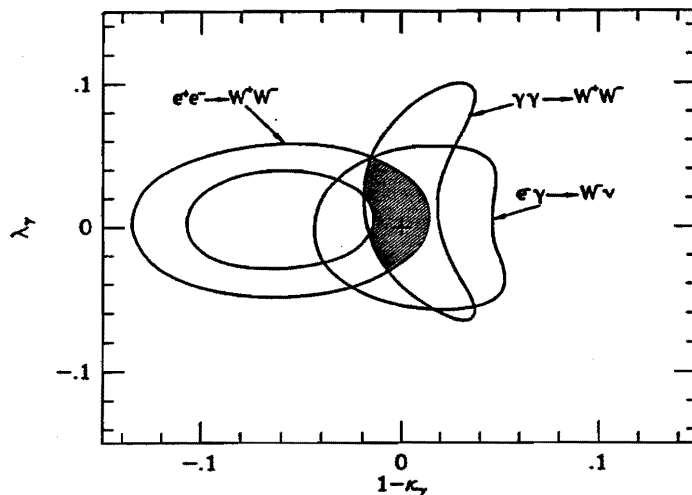


Figure 2.1 Combined constraint on γWW interactions (from Choi and Schrempp³⁵⁾).

used together at a 1/2 TeV collider provide greatly enhanced sensitivity to $\kappa_\gamma - 1$ and λ_γ . The constraints from $\gamma\gamma \rightarrow WW$ apply unambiguously to κ_γ and λ_γ , unlike $ee \rightarrow WW$ that also depends on κ_Z and λ_Z . Other interesting final states can be produced, often with larger cross sections than in e^+e^- annihilation. For instance,³⁶⁾ a charged Higgs scalar is produced with an asymptotic cross section that is six times larger,

$$R(\gamma\gamma \rightarrow H^+H^-) = \frac{3}{2}, \quad (2.7)$$

and the charged lepton asymptotic cross section is

$$R(\gamma\gamma \rightarrow L^+L^-) = 3 \ln \frac{s}{4M_L^2}. \quad (2.8)$$

It may also be possible to measure the $\gamma\gamma$ decay width of the standard model Higgs boson, $\Gamma(H \rightarrow \gamma\gamma)$, for certain values of the mass m_H . Gunion and Haber³⁷⁾ find observable signals for $\gamma\gamma \rightarrow H \rightarrow \bar{b}b$ if $70 \lesssim m_H \lesssim 150$ GeV and for $\gamma\gamma \rightarrow H \rightarrow ZZ$ if $200 \lesssim m_H \lesssim 250$ GeV. (An additional possible background to the $\bar{b}b$ signal from $\gamma\gamma \rightarrow \bar{c}c$ is under investigation.³⁸⁾) For the intermediate mass Higgs boson it may be possible at the SSC or LHC to measure the complementary quantity, $y_t^2 \cdot BR(H \rightarrow \gamma\gamma)$ where y_t is the ttH Yukawa coupling constant, in the process $gg \rightarrow \bar{t}tH$, $H \rightarrow \gamma\gamma$. Another constraint on y_t can be obtained in e^+e^- scattering, as discussed in Section 3 below.

$\Gamma(H \rightarrow \gamma\gamma)$ is a quantity of fundamental interest because it “counts” all quanta in the theory that have mass $\gtrsim O(m_H)$, that are electrically charged, and that obtain their mass from the Higgs boson. The amplitude $\mathcal{M}(H \rightarrow \gamma\gamma)$ is proportional to a conventionally defined quantity I , which for $m_b \ll m_H < M_W, m_t$ in the three generation standard model is given by W and t loop contributions³⁹⁾

$$I_3 = 7 - \frac{4}{3}R_t = \frac{47}{9} \quad (2.9)$$

where the W contributes 7 and $R_t = 4/3$ is the familiar R for $e^+e^- \rightarrow \gamma^* \rightarrow \bar{t}t$. However, for a fourth heavy generation we have $R_4 = 8/3$ and

$$I_4 = 7 - \frac{4}{3}(R_t + R_4) = \frac{15}{9}. \quad (2.10)$$

The cross section $\sigma(\gamma\gamma \rightarrow H)$ is then an order of magnitude smaller for four generations, and judging from the background estimates of Gunion and Haber the signal would probably not be observable.

Under these circumstances there is another “counting” process that could be studied at a very high energy $\gamma\gamma$ collider.⁴ Consider $\gamma\gamma$ scattering to a pair of longitudinally polarized Z bosons, $\gamma\gamma \rightarrow Z_L Z_L$. Suppose there is an ultraheavy electrically charged quantum X with spin 0 or $\frac{1}{2}$ that receives its mass from the standard model Higgs boson. Suppose further that

$$4m_X^2 \gg s \gg m_H^2, 4M_W^2. \quad (2.11)$$

(The condition $s \gg m_H^2$ is for convenience; the signal is bigger if it is relaxed.) The amplitude obtained from the Feynman diagram of figure 2.2a is then^{3,40)}

$$\mathcal{M}(\gamma\gamma \rightarrow Z_L Z_L) = \frac{\alpha R_X}{3\pi} \cdot \frac{s}{v^2}. \quad (2.12)$$

Equation (2.12) can be understood in terms of a low energy theorem for the $\gamma\gamma$ decay of a dilaton, $\sigma \rightarrow \gamma\gamma$, that follows from the trace anomaly,⁴¹⁾ with the Higgs boson interpreted as the dilaton and the coupling F_σ of the dilaton to the stress energy tensor replaced by the Higgs boson condensate v . The off-shell $\sigma\gamma\gamma$ amplitude for $\gamma\gamma$ center of mass energy \sqrt{s} is

$$\mathcal{M}(\sigma \rightarrow \gamma\gamma) = \frac{\alpha R}{3\pi F_\sigma} s \quad (2.13)$$

corresponding to

$$\mathcal{M}(H \rightarrow \gamma\gamma) = \frac{\alpha R_X}{3\pi v} s \quad (2.14)$$

in the present context.

The striking feature of equation (2.12) is the linear dependence on s : one factor of s from the form of the trace anomaly, proportional to $\alpha F_{\mu\nu} F^{\nu\mu}$, a second factor of s from the $H Z_L Z_L$ vertex, and a factor $1/s$ from the Higgs boson propagator with $m_H^2 \ll s$. The analogous amplitude for $gg \rightarrow Z_L Z_L$ was noted by Glover and van der Bij.⁴²⁾ This linear growth in s is not the usual “bad high energy behavior” that occurs in gauge theories when cancelling contributions are omitted. In particular, the box graph shown in figure 2.2b vanishes (decouples) in the limit of equation (2.11). Rather the triangle graph has “pseudo bad high energy behavior” that eventually decreases like m_X^2/s for $s > 4m_X^2$. There are indeed cancellations between figures 2.2a and 2.2b for $s > 4m_X^2$ but they only involve logarithmic dependence on s .⁴¹⁾

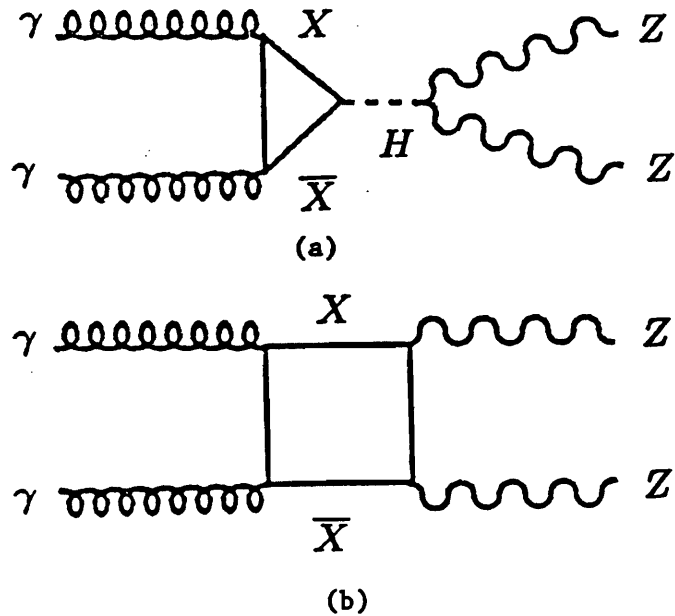


Figure 2.2 Feynman diagrams for $\gamma\gamma \rightarrow ZZ$.

A final theoretical remark before returning to practical matters: the equivalence theorem seems to imply a contradiction. Since the Hww vertex is constant rather than linear in s , figure (2.2a) only contributes a constant amplitude. The resolution is that equation (2.12) is instead recovered from the box graph (and its permutations) figure 2.2b! A factor of s arises from gauge invariance (requiring an $F_{\mu\nu} \cdot F^{\mu\nu}$ structure for the external photons) and the box does not decouple because the two $\bar{X}Xw$ vertices provide a factor m_X^2/v^2 to cancel the m_X^{-2} factor from the (finite) loop integral.⁴³⁾ Of course individual diagrams do not generally correspond between gauge and Goldstone boson amplitudes under the equivalence theorem, but this example is particularly amusing. First, the leading contribution is completely interchanged between the two diagrams in the two ways of doing the calculation. Second, the calculation is more easily done in terms of gauge bosons than Goldstone bosons, contrary to usual experience in which the Goldstone boson calculation is much simpler.

To return to the business at hand, the growing amplitude, equation (2.12),

implies a growing cross section,

$$\begin{aligned}\sigma(\gamma\gamma \rightarrow Z_L Z_L) &= \left(\frac{\alpha R_X}{24\pi^{3/2}}\right)^2 \frac{s}{v^4} \\ &= 0.36 \text{ fb} \cdot R_X^2 \cdot s(\text{TeV}^2).\end{aligned}\tag{2.15}$$

Since there is no tree approximation amplitude for $\gamma\gamma \rightarrow ZZ$, the background is determined by the Feynman diagrams of figure 2.2 with the W boson and the three known fermion generations in the loops. The background cross sections are proportional to $1/s$ and will therefore be negligible at high enough energy.

Suppose for example that X represents an ultraheavy fourth generation of quarks and leptons so that $R_X = 8/3$. For simplicity assume monochromatic photons with $\sqrt{s} = 1$ TeV and an integrated $\gamma\gamma$ luminosity of 100 fb^{-1} . To stay within the experimental acceptance and also because it improves the signal:background ratio, I impose an angular cut $|\cos\theta_Z| < 0.9$. The result is then 230 signal events and 5 background events. I have neglected the W loop contributions to the background (that would require a major effort to compute) and have also neglected the interference between the fourth and the three known generations in estimating the signal. Neither approximation is likely to effect the order of magnitude of the result.

However, in addition to the genuine ZZ background there is also the flood of WW events discussed above. They force us to the decays $ZZ \rightarrow \bar{\ell}\ell + (\bar{\ell}\ell/\bar{q}q)$, with $\ell = e, \mu, \text{ or } \tau$ i.e., one Z decays to a lepton pair while the second decays to a lepton or quark pair. The net branching ratio (with $\tau^+\tau^-\tau^+\tau^-$ omitted) is 0.15, leaving 35 signal events and 1 background event. This yield can be increased by as much as a factor 3 if $ZZ \rightarrow \bar{\nu}\nu + (\bar{\ell}\ell/\bar{q}q)$ provides an adequately clean signature, as I suspect it does, especially for events in which the observed Z boson has large transverse momentum. I am reconsidering the result for a realistic spectrum of $\gamma\gamma$ energies.³⁾

3. What we must find

As reviewed in section 1.1, the standard model implies that we must find Higgs bosons below or strong WW scattering above 1 TeV. In the latter case there will also be a complex spectrum of strongly interacting particles above 1 TeV. I will briefly describe the prospects to find and begin to study the Higgs

boson(s) and will present a very rough estimate of strong WW scattering signals for various e^+e^- collider energies.

3.1 STANDARD MODEL HIGGS BOSON

A light Higgs boson, say $m_H < 2M_W$, may be most easily found (with less luminosity) at lower energy e^+e^- colliders in $e^+e^- \rightarrow ZH$ — an example is discussed by Fujii.¹⁶⁾ I will focus here on colliders with $\sqrt{s} \geq 1$ TeV, in which WW fusion, $e^+e^- \rightarrow \bar{\nu}\nu H$ (figure 1.1), is typically the dominant production mechanism.

The SLAC study group²⁰⁾ has simulated the observation of a light Higgs boson with $m_H < 2M_W$ at a 1 TeV collider with 30 fb^{-1} . They consider WW fusion, $e^+e^- \rightarrow \bar{\nu}\nu H$, $H \rightarrow \bar{b}b$. The principal background, $e^+e^- \rightarrow e\nu W$, $W \rightarrow \bar{q}q$, is shown in figure 3.1a. The signals after cuts for 120 and 150 GeV Higgs bosons are shown with an expanded vertical axis in figure 3.1b. It is clear from the figure that this technique will be much more difficult if not impossible for $60 \lesssim m_H \lesssim 90$ GeV. Fujii shows in his talk¹⁶⁾ that this case can be covered at a lower energy collider using $e^+e^- \rightarrow ZH$. At the LHC or SSC the Higgs boson in this mass range can be discovered with $gg \rightarrow \bar{t}tH$, $H \rightarrow \gamma\gamma$, providing a measurement of $y_t^2 \cdot BR(H \rightarrow \gamma\gamma)$ where y_t is the ttH Yukawa coupling constant.⁴⁴⁾

For $m_H > 2M_Z$ the Higgs boson width is dominated by

$$\Gamma(H \rightarrow WW + ZZ) \cong 0.5 \text{ TeV} \cdot m_H^3 (\text{TeV}). \quad (3.1)$$

We discuss first the narrow width case, $\Gamma_H \ll m_H$, for which the signal has a recognizable peak. For m_H approaching ~ 1 TeV we have $\Gamma_H \cong O(m_H)$ so that the resonance peak is lost. Detection is then much more difficult. Both the experimental issues and the underlying physics begin to merge with the case of strong WW scattering, to be discussed in subsection 3.2.

The narrow Higgs boson decaying to $WW + ZZ$ can be readily discovered, at the SSC or LHC in clean leptonic final states,⁴⁵⁾ or at an e^+e^- collider of sufficient energy in the four jet final state. At e^+e^- colliders with $\sqrt{s} > 1$ TeV the dominant mechanism is WW fusion,

$$e^+e^- \rightarrow \bar{\nu}\nu H, H \rightarrow WW \rightarrow \bar{q}q\bar{q}q.$$

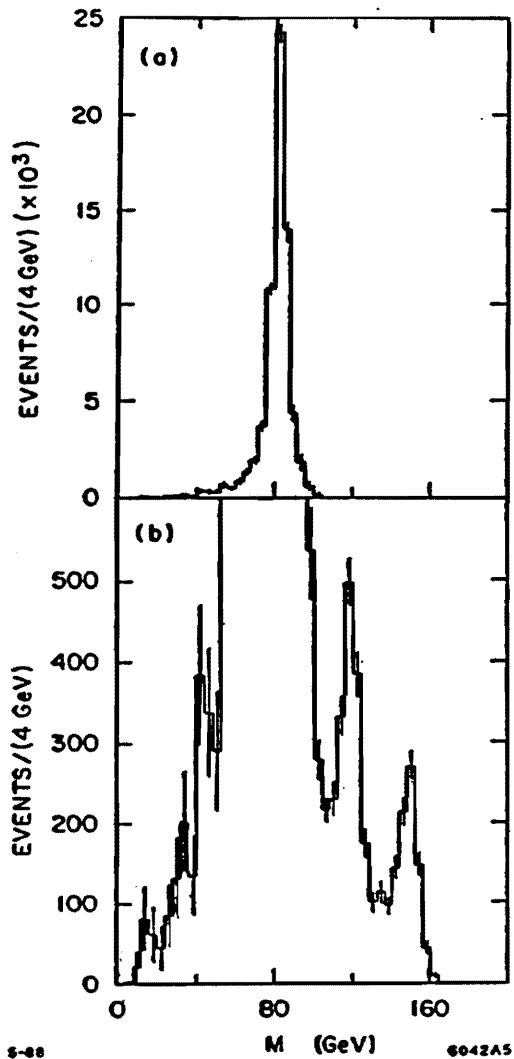


Figure 3.1 (a) Background to $e^+e^- \rightarrow \bar{\nu}\nu H$ from $e^+e^- \rightarrow e\nu W$. (b) Background plus signals for 120 and 150 GeV Higgs bosons (from reference 20).

The largest backgrounds are from bremsstrahlung photons, $\gamma\gamma \rightarrow WW$, and from beamstrahlung followed by $e^+e^- \rightarrow WW$ at reduced energy. A strategy against these backgrounds was developed at the CLIC La Thuile study.⁴⁶⁾ High p_T bremsstrahlung photons are eliminated by a veto on events containing visible electrons, e.g., Kurihara⁴⁷⁾ vetos events with electrons of energy $E_e > 50$ GeV and $\theta_e > 9^\circ$. The surviving $\gamma\gamma \rightarrow WW$ events and most of the beamstrahlung $e^+e^- \rightarrow WW$ events are then eliminated by requiring $p_T(WW) > p_{TMIN}$ with p_{TMIN} chosen in a range from $\sim M_W/2$ to M_W . Most signal events pass this

cut since in WW fusion the Higgs boson is produced with a p_T distribution of order M_W due to the initial state, virtual W bosons. Kurihara⁴⁷⁾ reported, using this strategy, that with 60 fb^{-1} Higgs boson detection is possible at least to $m_H \lesssim \frac{1}{2}\sqrt{s}$. His simulation for a 500 GeV Higgs boson at a 1 TeV collider is shown in figure 3.2. Similar conclusions were reached by the SLAC study group using a different though related strategy.

In his talk Fujii¹⁶⁾ describes a more recent, still unpublished study by Kurihara⁴⁸⁾ of the 1 TeV Higgs boson that includes two additional backgrounds, $\gamma W \rightarrow WZ$ and $\sigma(m_H \rightarrow 0)$, discussed in section 3.2 below. A surprising result of Kurihara's analysis is the large number of $e^+e^- \rightarrow WW$ events that pass the cuts. I do not understand the origin of these events but suspect they may arise from initial state radiation with $p_T > p_{TMIN}$ followed by $e^+e^- \rightarrow WW$. Narrow Higgs boson signals should be reconsidered including these two additional backgrounds and the high p_T component of $e^+e^- \rightarrow WW$.

With our current fixation on finding the Higgs boson, it is easy to forget that discovery will only be the beginning. If a narrow Higgs boson is discovered in WW fusion with decay to $WW+ZZ$, we will know nothing about its coupling to fermions. We will then want to measure the largest Yukawa coupling, that of

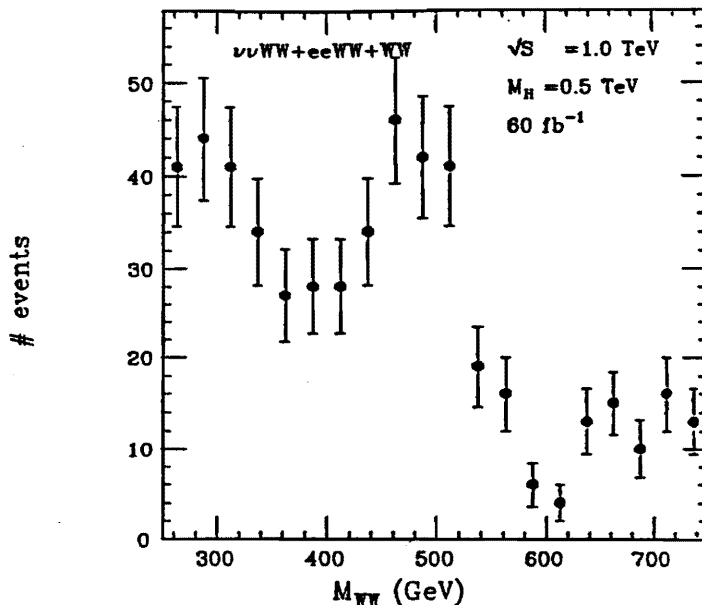


Figure 3.2 Signal for 500 GeV Higgs boson at a 1 TeV collider with 60 fb^{-1} (from reference 47).

at low energy. For instance, $W^+W^- \rightarrow ZZ$ is constructed from a_{00} and a_{20} , and $W^+W^- \rightarrow W^+W^-$ from a_{11} and a_{20} . The model for $|a_{00}|$ is

$$|a_{00}| = \frac{s}{16\pi v^2} \theta(16\pi v^2 - s) + 1 \cdot \theta(s - 16\pi v^2), \quad (3.6)$$

shown in figure 3.4.

Other models may have larger or smaller amplitudes. Hikasa and Igi⁵³⁾ have applied the N/D method to the theory of the ultraheavy Higgs boson. The resulting $J = 0$ amplitude is considerably bigger than the linear model. Barger et al⁵⁴⁾ used the K -matrix to satisfy the low energy theorems and unitarity. The K -matrix model for the $I = J = 0$ partial wave is

$$a_{00} = \frac{s}{16\pi v^2} \left(1 + i \frac{s}{16\pi v^2} \right)^{-1} \quad (3.7)$$

which is smaller than the linear model.

It is instructive to compare the linear model with pion scattering data.

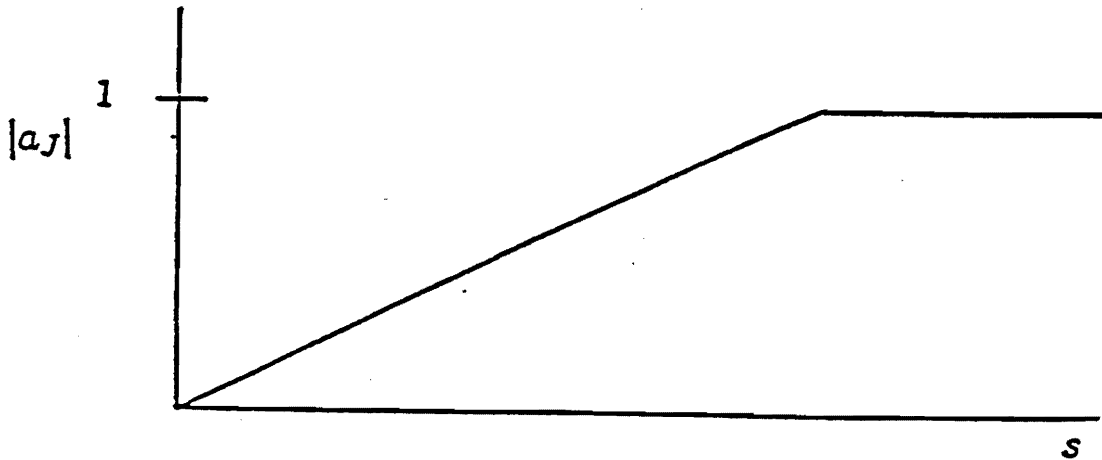


Figure 3.4 The linear model for $|a_{00}|$.

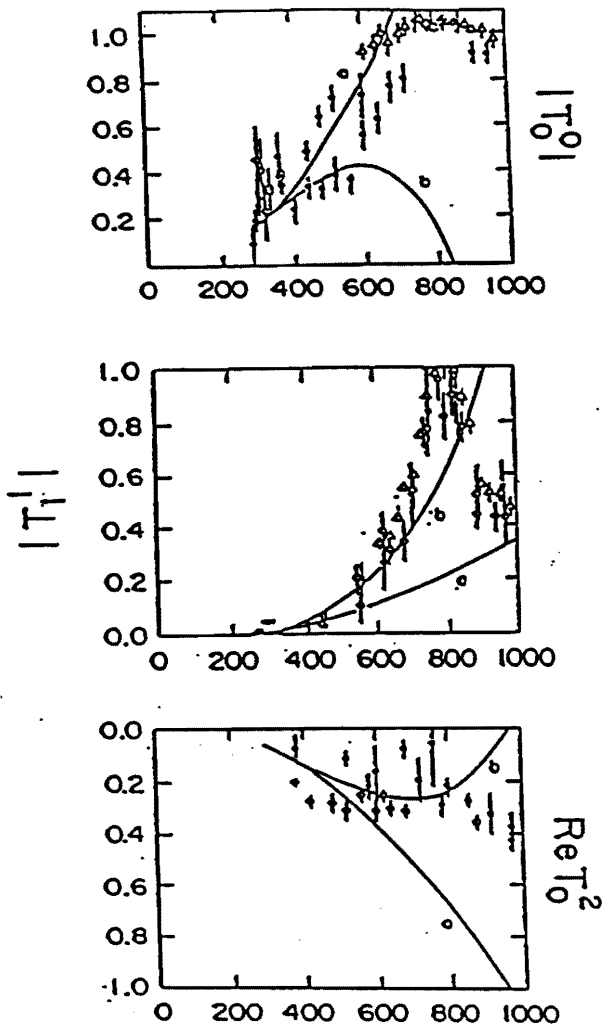


Figure 3.5 Comparison of the linear model (curves a) with pion-pion scattering data (from reference 55).

Figure 3.5 is a compilation of $\pi\pi$ scattering data for $|a_{00}|$, $|a_{11}|$, and $Re a_{20}$ from Donoghue et al.⁵⁵⁾ (a_{20} is almost purely real in this energy region since it is an exotic channel in QCD). The linear model is represented by the curves labeled a. We see that it is a surprisingly good fit to the data for $|a_{00}|$ (even in the region of unitarity saturation above 700 MeV where $|a_{00}| \cong 1$), that it badly underestimates $|a_{11}|$ because of the $\rho(770)$, and that it describes a_{20} pretty well up to about ~ 600 MeV (corresponding to ~ 1.6 TeV in \mathcal{L}_{SB}).

Detection of Strong Scattering

Detection of strong scattering is very difficult: there is no recognizable

the top quark, to see if it has the standard model value

$$y_t = \frac{em_t}{2 \sin \theta_W M_W}. \quad (3.2)$$

At the SSC or LHC this can be done indirectly by extracting the $gg \rightarrow H$ component of the H production cross section, since in the standard model with three generations $gg \rightarrow H$ is determined by the top quark loop contribution. More direct measurement of y_t is possible at an e^+e^- collider if and only if ⁴⁹⁾ the Higgs boson can be produced and is heavy enough to decay to $t\bar{t}$. Two simulations have been performed. Tauchi, Fujii, and Miyamoto⁵⁰⁾ considered $m_H = 300$ GeV with $m_t = 130$ GeV. For 120 fb^{-1} at a 600 GeV collider using $e^+e^- \rightarrow ZH, H \rightarrow t\bar{t}$, they obtain a 20% determination of y_t . Their result is shown in figure 3.3. Tsukamoto⁵¹⁾ considered WW fusion, $e^+e^- \rightarrow \bar{\nu}\nu H, H \rightarrow t\bar{t}$, with $m_H = 600$ GeV and $m_t = 150$ GeV. He found that a 20% measurement of y_t requires 300 fb^{-1} at a 1 TeV collider or 60 fb^{-1} at a 1.5 TeV collider. The 1.5 TeV collider provides a four times larger signal and a two times smaller background than the 1 TeV collider. This is further evidence of the critical importance of energy in the WW fusion process as discussed in Section 1.2. A similar conclusion applies to pp colliders, where TeV WW fusion signals tend to increase approximately

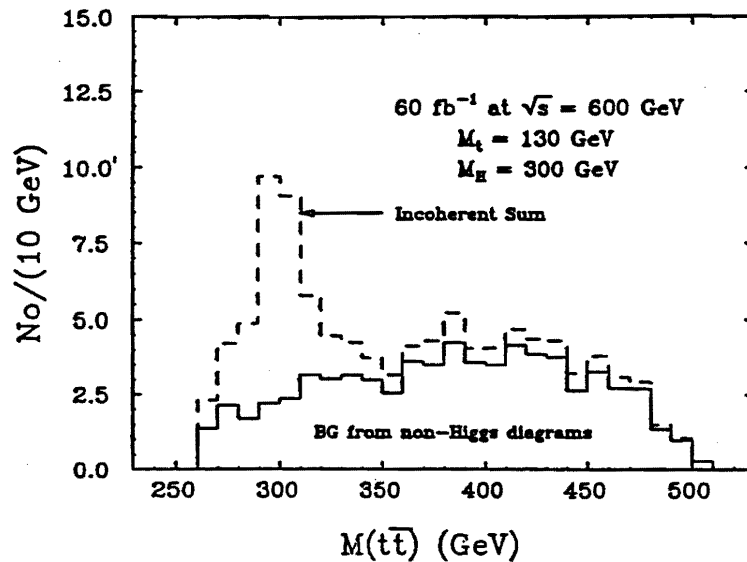


Figure 3.3 $H \rightarrow t\bar{t}$ for 300 GeV Higgs boson at a 600 GeV collider with $m_t = 130$ GeV and assuming 60 fb^{-1} (from reference 50).

like the square of the collider energy while the backgrounds are approximately linear.^{51a)}

3.2 STRONG WW SCATTERING

If the symmetry breaking sector is strongly coupled and has no light quanta other than W_L^\pm and Z_L , then there will be strong WW scattering at $s_{WW} > 1$ TeV². In that case we can only guess at the specific dynamics and spectrum of the new strong interaction lagrangian \mathcal{L}_{SB} . However we know in general that strong WW scattering must be consistent with the low energy theorems and with unitarity, discussed in section 1.1. The low energy theorems relevant for e^+e^- collider experiments are⁸⁾

$$\mathcal{M}(W_L^+W_L^- \rightarrow Z_LZ_L) = \frac{1}{\rho} \frac{s}{v^2} \quad (3.3)$$

$$\mathcal{M}(W_L^+W_L^- \rightarrow W_L^+W_L^-) = -(4 - \frac{3}{\rho}) \frac{u}{v^2}, \quad (3.4)$$

valid in the domain $M_W^2 \ll s \ll \min\{M_{SB}^2, (4\pi v)^2\}$. For WW scattering at the SSC/LHC and also for e^+e^- colliders of up to a few TeV, elastic unitarity is a good approximation to the general unitarity constraint,

$$\text{Im } a_J = |a_J|^2, \quad (3.5)$$

that implies $|\text{Re } a_J| < \frac{1}{2}$ and $|a_J| \leq 1$ (both also valid in the inelastic region).

Gaillard and I considered a simple linear model that satisfies these constraints and provides order of magnitude estimates of strong WW scattering signals.⁶ The model is conservative in the sense that much larger signals will occur if, as we expect, resonances occur in at least some channels. The linear model extrapolates the low energy theorem amplitude, regarded as a model for the *absolute* value of each partial wave amplitude up to the energy at which $|a_J| = 1$, beyond which it is assumed to remain at $|a_J| = 1$. The actual construction involves decomposing the physical amplitudes such as equations (3.3) and (3.4) into partial wave amplitudes a_{IJ} where I denotes the custodial isospin⁵²⁾ that is necessarily⁸⁾ a good symmetry of the longitudinal W boson interactions

structure and the rates are much smaller than for narrow Higgs bosons. There are two other important backgrounds in addition to the $\gamma\gamma \rightarrow WW$ and $e^+e^- \rightarrow WW$ backgrounds discussed in connection with the narrow Higgs boson. First is $\gamma W \rightarrow ZW$, that is not eliminated by the combination of e^- veto and $p_T(WW)$ cut, since the electron from the nearly real photon disappears along the beam direction while the neutrino from the virtual W carries off transverse momentum of order M_W . The second additional background is the W^+W^- or ZZ cross section from the light Higgs boson (e.g., $m_H \rightarrow 0$) version of the standard model, i.e., $W_T W_T$ (transverse-transverse) and $W_T W_L$ (transverse-longitudinal) boson pairs that result from the $SU(2)_L \times U(1)_Y$ gauge interactions and are essentially independent of the symmetry breaking sector \mathcal{L}_{SB} .

A complete tree approximation calculation of the signals and backgrounds has been made by Hagiwara, Kanzaki, and Murayama⁵⁶ (omitting s -channel gauge boson exchanges that contribute at most several percent⁵⁷). They consider a $\sqrt{s} = 1.5$ TeV collider and propose the following cuts:

- a) e^\pm veto as in the narrow Higgs boson study discussed above⁴⁷)
- b) $p_T(WW) > 50$ GeV
- c) $|\cos \theta_V| < 0.6$ for $V = W$ or Z
- d) $M_{VV} > 500$ GeV

They compute the strong WW scattering signal by taking the difference of the $m_H \rightarrow \infty$ and $m_H \rightarrow 0$ limits of the standard model,

$$\sigma_{Strong} = \sigma_{SM}(m_H \rightarrow \infty) - \sigma_{SM}(m_H \rightarrow 0). \quad (3.8)$$

Provided Γ_H is held fixed as $m_H \rightarrow \infty$ and that unitarity is treated correctly, equation (3.8) is equivalent to the linear model⁶ described above. (An earlier study⁵⁸) of strong WW scattering at e^+e^- colliders overestimated the signal and underestimated background because the signal was identified with $\sigma(m_H \rightarrow \infty)$ without subtracting the $\sigma(m_H \rightarrow 0)$ component.)

The result of HKM⁵⁶) with cuts a) - d) and $\sqrt{s} = 1.5$ TeV is

$$\sigma_{Strong}(ZZ) = 0.74 - 0.37 = 0.37 \text{ fb} \quad (3.9)$$

$$\sigma_{Strong}(WW) = 0.68 - 0.45 = 0.23 \text{ fb} \quad (3.10)$$

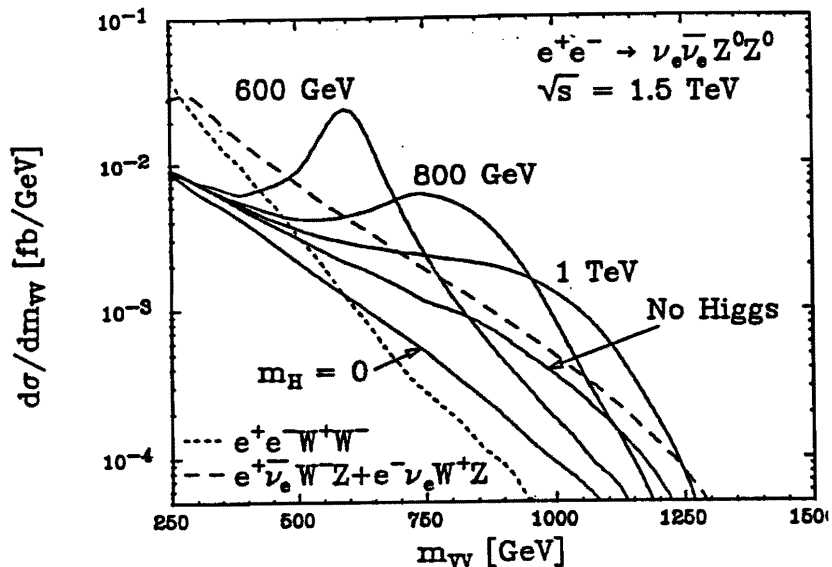


Figure 3.6 Strong scattering (“No Higgs”) and Higgs boson signals and various backgrounds (from reference 56).

where the differences $\sigma(m_H \rightarrow \infty) - \sigma(m_H \rightarrow 0)$ are displayed explicitly. The cuts a) - d) reduce the WZ background to a level that I estimate from figure 3.6 (taken from reference 56) at about ~ 1.2 fb. Further reduction of the WZ background depends on the jet-jet mass resolution for M_W and M_Z and requires simulation. HKM do not include the large $e^+e^- \rightarrow WW$ background found in the study of Kurihara⁴⁸⁾ reported by Fujii.¹⁶⁾

Since equation (3.8) is equivalent to the linear model, it should be possible to check the results in equations (3.9) and (3.10) against a calculation using the equivalence theorem, the effective W approximation (EWA) and the linear model.⁶⁾ In order to include the cut on $p_T(WW)$ I have use the EWA (which has $p_T(WW) = 0$) but with $p_T(WW)$ smeared using a fit⁵⁹⁾ to the tree-approximation $p_T(WW)$ distribution. My results are 0.44 fb and 0.23 fb for ZZ and WW respectively. The good agreement with equations (3.9) and (3.10) is a deep consistency check of both calculations.

To guess at the size of the detectable signal for various collider energies, I have made a crude estimate of the experimental acceptance in the four jet final

	WW	ZZ
Branching ratio	0.67 ²	0.71 ²
Detector	(0.57 to 0.85) ²	
Losses from beamstrahlung + initial state radiation	~ $\frac{1}{2}$	
Net acceptance	0.07-0.16	0.08-0.18

Table 3.1 A crude estimate of the net acceptance for WW and $ZZ \rightarrow \bar{q}q + \bar{q}q$.

state. The relevant factors are shown in table 3.1. The reconstruction efficiency for $W \rightarrow \bar{q}q$, 0.57 - 0.85, is abstracted from two studies^{20,29)} of $e^+e^- \rightarrow WW$, but should really be based on a simulation of strong WW scattering. In such a simulation the reconstruction efficiency for W and $Z \rightarrow \bar{q}q$ will be constrained by the need for sufficient accuracy in $M_{\bar{q}q}$ to reject the WZ background. The factor $\sim 1/2$ reduction from beamstrahlung and initial state radiation is a guess based on the extreme sensitivity of the signal to the actual e^+e^- collision energy, as shown in table 3.2 for collision energies between 1.0 and 1.5 TeV. As emphasized in section 1.3, the actual beamstrahlung spectrum depends on the design of the linear collider. The final guess for the net acceptance in table 3.1 ranging from 0.07 - 0.16 for WW and 0.08 - 0.18 for ZZ , is probably reasonable but should be replaced with a simulation study including beamstrahlung and initial state radiation. Kurihara's⁴⁸⁾ first effort at such a simulation for the 1 TeV Higgs boson signal is described in Fujii's talk.¹⁶⁾

\sqrt{s} (TeV)	1 TeV Higgs Boson	Linear Model
1.0	0.1	0.2
1.1	0.2	0.3
1.2	0.3	0.4
1.3	0.5	0.6
1.4	0.7	0.8
1.5	1.0	1.0

Table 3.2 Cross section after cuts for $WW + ZZ$ normalized to 1 at $\sqrt{s} = 1.5$ TeV.

\sqrt{s} (TeV)	1 TeV Higgs Boson	Linear Model
1.0	1 - 2	0.5 - 1
1.5	10 - 22	2 - 5
2.0	25 - 60	6 - 13
3.0	60 - 140	16 - 36
5.0	105 - 240	37 - 83
10.0	150 - 340	70 - 160

Table 3.3 Number of $WW + ZZ$ signal events per $50fb^{-1}$ for HKM cuts and assuming the range of acceptances from table 3.1.

Table 3.3 displays the sum of the WW and ZZ signals for collider energies from $\sqrt{s} = 1$ to 10 TeV. (It's much easier being a theorist than an accelerator physicist!) Results are presented for the 1 TeV Higgs boson and for the linear strong scattering model. The calculations use the equivalence theorem with the p_T -smeared effective W approximation as described above. Yields are in events per $50 fb^{-1}$ with the HKM⁵⁶⁾ cuts a) - d) defined in the preceding discussion. The range of values in each entry reflects the range of acceptances in table 3.1.

We can get a preliminary idea of the size of the backgrounds from Kurihara's study as reported here by Fujii.¹⁶⁾ Scaling his results to correspond to $50 fb^{-1}$, the signal for the 1 TeV Higgs boson at a 1.5 TeV collider would be 17 events in $H \rightarrow W^+W^-$, in agreement with the upper end of the estimate in table 3.3 for $\sqrt{s} = 1.5$ TeV (that also includes ZZ events). The corresponding background from Kurihara's study is 53 events of which 17 are from the standard model cross section, $\sigma(m_H \rightarrow 0)$, and 27 are $e^+e^- \rightarrow WW$ events at reduced energy. While the precise cuts used by Kurihara differ from the HKM cuts we have

	$ZZ \rightarrow \bar{\ell}\ell + \bar{\ell}\ell/\bar{\nu}\nu$		$W^+W^+ \rightarrow \ell^+\nu\ell^+\nu$
	1 TeV Higgs	Linear Model	Linear Model
Signal	100	27	37
Background	43	30	13

Table 3.4 Signal events per $10fb^{-1}$ at the SSC.

used here, the signal:background ratio is probably similar. Including also the $\sigma_{ZZ}(m_H \rightarrow 0)$ background (that contributes little to Kurihara's analysis since he considers only the W^+W^- signal), it seems that the background is at least twice as big as the 1 TeV Higgs boson signal and several times larger than the strong scattering signal. (The background to strong WW scattering in the $W^+W^- + ZZ$ final state will be larger than the numbers quoted from Kurihara's study, because he requires $0.5 < M_{WW} < 1$ TeV, and because his focus on the W^+W^- signal greatly reduces the $\sigma_{ZZ}(m_H \rightarrow 0)$ and the $\gamma W \rightarrow ZW$ backgrounds.) It then seems that with 50 fb^{-1} a 2 to 3 TeV collider would be needed to see a solid ($\sim 5\sigma$) signal for the 1 TeV Higgs boson, while 3 to 5 TeV might be needed to measure strong WW scattering. With sufficiently higher luminosity lower energies could suffice.

These are clearly very rough guesses that should be replaced by simulations relevant to the particular processes and collider energies. In particular I have used the HKM cuts for all collider energies even though they were proposed only for $\sqrt{s} = 1.5$ TeV. At higher energy the relationship of signal and background will change, and different cuts may be more effective. Studies of strong WW scattering for the SSC also suggest that a combined cut on M_{WW} and p_{Tj} may be more effective than just cutting on M_{WW} , since the p_{Tj} cut tends to enhance the longitudinal W signal over transverse W backgrounds.⁶⁰⁾

For comparison table 3.4 shows $W^+W^{+60)}$ and $ZZ^{61)}$ strong scattering signals and backgrounds for the SSC in events per 10 fb^{-1} . (The ZZ signals and backgrounds for the 1 TeV Higgs boson were computed in parallel with the strong scattering signal of reference 61 but were not published.) The quoted event yields incorporate estimates for experimental acceptance, but are incomplete in the sense that additional potential backgrounds require further study in both cases.

Strong interaction resonances: techni-rho

If \mathcal{L}_{SB} is strongly interacting we eventually expect bigger signals than the linear model, just as the $\rho(770)$ enhances the a_{11} amplitude in $\pi\pi$ scattering, figure 3.5. A strong \mathcal{L}_{SB} need not resemble QCD, but technicolor models will be very similar. For instance, in the one generation $SU(4)_{TC}$ model we expect a $J = 1$ ρ_T resonance with mass $m \cong 0.3$ TeV, decaying strongly to pairs of longitudinally polarized W and Z bosons. Iddir et al.⁶²⁾ have examined whether

the $\rho_T(1.8)$ produces observable final state interactions at a 1 TeV collider in $e^+e^- \rightarrow W^+W^-$. They find that the interference effects between the ρ_T and the background amplitudes are probably unobservably small because $W_L^+W_L^-$ is only large in the backward hemisphere, whereas the region in which the $J = 1$ and $J > 1$ partial waves are comparable and can therefore interfere significantly is near $\theta = 0$.⁶³⁾ However for a collider able to produce the ρ_T , $\sqrt{s} = m = 1.8$ TeV, the effect is quite large. For scattering into the backward region $3\pi/5 < \theta < 4\pi/5$ Iddir et al. find 700 signal events and only 70 background events with a year of running at $10^{33} \text{ cm}^{-2} \text{ sec}^{-1}$.

A clean signal for $\rho_T(1.8)$ can be observed at the SSC but not with enough events for detailed studies. For instance, with 10 fb^{-1} there are 19 signal and 2 background events for $\rho_T \rightarrow WZ \rightarrow \ell\nu + \bar{\ell}\ell$ where $\ell = e$ or μ .^{51a)}

4. Conclusions: e^+e^- and pp colliders

The old clichés about e^+e^- and pp physics are still largely valid in the TeV energy region. The multi-TeV pp colliders have tremendous reach for new physics and some capability for detailed studies but with significant blind spots. High luminosity TeV e^+e^- colliders can cover the blind spots of the pp colliders and will be the facilities of choice for detailed study of the new phenomena that must be discovered in or below the TeV energy region. Together pp and e^+e^- colliders provide a powerful, highly complementary approach to the new physics.

Consider for instance a 40 TeV pp collider. With 10 fb^{-1} it probes the full range of electroweak symmetry breaking including Higgs bosons to 1 TeV, strong WW scattering above 1 TeV, and strong WW resonances such as the techni-rho to 2.5 TeV. It can search for supersymmetry over the full range that is pertinent if SUSY is relevant to the electroweak scale, including squarks to at least 1 TeV and gluinos to 2 TeV. It can search for heavy quarks to at least 1 TeV and can discover Z' bosons as heavy as 8 TeV. This represents unique exploratory reach that promises to take us to the next step beyond the standard model.

High luminosity TeV e^+e^- colliders also have tremendous potential for discoveries and for detailed studies. They would cover the blind spots of the pp colliders, such as heavy charged leptons, heavy Majorana neutrinos, leptonic su-

perparticles, the supersymmetric Higgs sector, and the study of on-shell Yukawa couplings in $H \rightarrow \bar{t}t$. They retain unique capability for the physics of the $J = 1$ channel, such as Z' and ρ_T . Favorable signal:background conditions and linear polarization make them facilities of choice to begin the detailed study of whatever we find when we take the first step beyond the standard model.

What we are actually able to accomplish depends critically on progress in very challenging areas of accelerator physics, arguably the most important subdiscipline for the future of high energy physics. Before fixing the design parameters of the first $\sqrt{s} \geq 1$ TeV e^+e^- colliders, it will be helpful to have viewed the landscape of TeV physics from the SSC/LHC. The selection of physics goals and choice of design parameters will be aided by knowledge of specific physics targets obtained from the exploratory experiments at the pp colliders. For the next twenty years as for the last twenty, we need both e^+e^- and pp physics to go forward. We will succeed best by continuing to work together to find and explore the new physics.

Acknowledgements: I have many people to thank for providing materials and for helpful discussions, including T. Barklow, S. Drell, M. Einhorn, K. Fujii, M.K. Gaillard, J.D. Jackson, S. Kawabata, Y. Kurihara, A. Miyamoto, H. Murayama, M. Peskin, and A. Sanda. I also wish to thank the Conference Secretary T. Matsui and the KEK staff for the efficient organization of an excellent meeting and for their kindness and hospitality.

References

1. I. Ginzburg et al., *Pizma v. ZhETF* **34:514**, 1981; *Nucl. Instr. and Meth.* **205:47** 1983; **219:5**, 1984; *Y. Fizika* **38,2:372**, 1983; C. Akerlof, U. Michigan preprint UMHE 81-59, 1981; A. Skrinsky, *U. Fiz. Nauk* **138:3**, 1982; J. Sens, *Proc. 8th Int. Workshop on Photon-Photon Collisions*, ed. U. Karshon, Shores, 1988 (World Scientific, Singapore); T. Barklow, *Proceedings of 1990 DPF Summer Study, Snowmass*; V. Telnov, *Nucl. Instr. Meth.* **A294:72**, 1990.
2. J. Ballam et al., *Phys. Rev. Lett.* **23:498**, 1969; **24:960**, 1975; *Phys. Rev.* **D5:545**, 1972.
3. M. Chanowitz, to be submitted for publication.

4. M. Chanowitz, *Ann. Rev. Nucl. Part. Sci.* **38:323**, 1988.
5. J.M. Cornwall, D. Levin, G. Tiktopoulos, *Phys. Rev.* **D10:1145**, 1974.
6. M. Chanowitz, M. Gaillard, *Nucl. Phys.* **B261:379**, 1985.
7. G. Gounaris, R. Kögerler, H. Neufeld, *Phys. Rev.* **D34:3527**, 1986; D. Soper and Z. Kunszt, *Nucl. Phys.* **B296:253**, 1988; J. Bagger and C. Schmidt, *Phys. Rev.* **D41:264**, 1990; H. Veltman, *Phys. Rev.* **D41:2294**, 1990.
8. M. Chanowitz, M. Golden, H. Georgi, *Phys. Rev.* **D36:1490**, 1987; *Phys. Rev. Lett.* **57:2344**, 1986.
9. S. Weinberg, *Phys. Rev. Lett.*, **17:616**, 1966.
10. M. Chanowitz, M. Gaillard, *Phys. Lett.* **B142:85**, 1984 and ref. 6; S. Dawson, *Nucl. Phys.* **B249:42**, 1985; G. Kane, W. Repko, W. Rolnick, *Phys. Lett.* **B148:367**, 1984.
11. V. Baier, V. Katkov, *Phys. Lett.* **A25:492**, 1967.
12. R. Jacobsen et al., SLAC-PUB 5205, 1990; T. Tauchi et al., KEK 90-181 and Proc. Snowmass '90.
13. M. Drees, R. Godbole, *Phys. Lett.* **B257:425**, 1991.
14. F. Halzen, C. Kim, M. Strong, MAD/PH/673, 1991.
15. R. Blankenbecler, S. Drell, *Phys. Rev. Lett.* **61:2324**, 1988.
16. K. Fujii, these proceedings.
17. S. Iwata, KEK preprint 91-9, 1991 (to be published in Proc. Second JLC Workshop).
18. R. Cahn et al., *Phys. Rev.* **D35:1626**, 1987; R. Kleiss, W. Stirling, *Phys. Lett.* **200B:193**, 1988; V. Barger et al., *Phys. Rev.* **D44:1426**, 1991.
19. M. Veltman, *Nucl. Phys.* **B123:89**, 1977. M. Chanowitz, M. Furman, I. Hinchliffe, *Nucl. Phys.* **B153:402**, 1979; *Phys. Lett.* **78B:285**, 1978.

20. C. Ahn et al., SLAC-329, 1988.
21. W. Buchmüller, C. Greub, Nucl. Phys. **B363:345**, 1991.
22. S. Dawson et al., p. 144, *Proc. Workshop on Experiments, Detectors and Experimental Areas for the SSC*, July, 1988, Berkeley, eds. R. Donaldson and M. Gilchriese (World Scientific, Singapore, 1988).
23. V. Barger, T. Han, J. Ohnemus, PRD**37:1174**, 1988; I. Hinchliffe, Int. J. Mod. Phys. A **4:3867**, 1989.
24. J. Gunion et al., Phys. Rev. **D38:3444**, 1988.
25. E. Eichten, K. Lane, M. Peskin, Phys. Rev. Lett. **50:811**, 1983.
26. See for instance M. Peskin, SLAC-PUB-3496, 1984. I am not aware of simulation studies of the experimental sensitivity to Λ in TeV e^+e^- collisions.
27. V. Barnes et al., p. 235, reference 40.
28. K. Hagiwara et al., Nucl. Phys. **B282:253**, 1987.
29. A. Miyamoto, KEK 90-188, to be published in Proc. Second JLC Workshop.
30. G. Kane, J. Vidal, C. Yuan, Phys. Rev. **D29:945**, 1984.
31. E. Yehudai, Phys. Rev. **D41:33**, 1990.
32. H. Georgi, Nucl. Phys. **B361:339**, 1991.
33. K. Fujii, to be published in Proc. Second JLC Workshop.
34. M. Chanowitz, in *Photon-Photon Collisions*, p. 205, ed. U. Karshon (World Scientific, 1988).
35. S. Choi, F. Schrempp, Phys. Lett. **B272:149**, 1991; E. Yehudai, Phys. Rev. **D44:3434**, 1991.
36. V. Telnov, reference 1.

37. J. Gunion, H. Haber, SCIPP 90/22, to be published in Proc. 1990 Snowmass DPF Summer Study.
38. P. Zerwas, work in progress.
39. J. Ellis, M. Gaillard, D. Nanopoulos, Nucl. Phys. **B106:292**, 1976; M. Shifman et al., Sov. J. Nucl. Phys. **30:711**, 1979.
40. Similar results apply to $gg \rightarrow Z_L Z_L$. The experimental implications at pp colliders are under study.
41. R. Crewther, Phys. Rev. Lett. **28:1421**, 1972; M. Chanowitz, J. Ellis, Phys. Lett. **40B:397**, 1972; Phys. Rev. **D7:2490**, 1973.
42. E. Glover, J. van der Bij, Nucl. Phys. **B321:561**, 1989; M. Berger, M. Chanowitz, LBL 31343, 1991 (submitted for publication).
43. I have found a simple verification that the box graph gives the leading result in the limit of equation 2.11 in the Goldstone boson formulation.
44. J. Gunion, Phys. Lett. **B261:510**, 1991; W. Marciano, F. Paige, Phys. Rev. Lett. **66:2433**, 1991.
45. Solenoidal Detector Collaboration, E.L. Berger et al., Letter of Intent, SDC-90-00151, 1990.
46. B. Mele, p. 13, Vol. II, *Proc. of the Workshop on Future Accelerators*, ed. J. Mulvey, La Thuile, 1987, CERN 87-07; F. Richard, *ibid*, p.23.
47. Y. Kurikara, p. 195, *Proc. of the First Workshop on Japan Linear Collider*, 1989, ed. S. Kawabata, KEK 90-2.
48. Y. Kurihara, presented at the Lapland meeting on TeV linear colliders.
49. K. Hagiwara, H. Murayama, I. Watanabe, KEK-TH-264, 1990.
50. T. Tauchi, K. Fujii, A. Miyamoto, to be published in *Proc. Second JLC Workshop*.
51. T. Tsukamoto, *op cit*.

- 51a. M. Chanowitz, report to DOE (Drell) panel on SSC energy (unpublished).
52. P. Sikivie et al., Nucl. Phys. **B173:189**, 1980.
53. K. Hikasa, K. Igi, Phys. Rev. **D261:285**, 1991.
54. V. Barger et al., Phys. Rev. **D42:3052**, 1990.
55. J. Donoghue, C. Ramirez, G. Valencia, Phys. Rev. **D38:2195**, 1988.
56. K. Hagiwara, J. Kanzaki, H. Murayama, DTP 91/18.
57. Y. Kurihara, private communication.
58. J. Gunion, A. Tofighi-Niaki, Phys. Rev. **D36:2671**, 1987.
59. R. Cahn, S. Ellis, W. Stirling, Phys. Rev. **D35:1626**, 1987.
60. M. Berger, M. Chanowitz, Phys. Lett. **263B:509**, 1991.
61. M. Berger, M. Chanowitz, LBL 31343, 1991.
62. F. Iddir et al., Phys. Rev. **D41:22**, 1990.
63. See however B. Holdom, Phys. Lett. **258B:156**, 1991, who finds an observable strong scattering correction in $e^+e^- \rightarrow WW$ at $\sqrt{s} = 1$ TeV using an effective lagrangian based on QCD.